小山工業高等専門学校研究紀要
第 41 号 (2009) 57－ 64

The Application of Wavelet Transform to Identify Chaotic Vibration

Qin Zhu
Dept. of Mechanical Engineering
Oyama National College of Technology
zhu@oyama-ct.ac.jp

Shan Liang
Automation Academy
Chongqin University
lightsun@cqu.edu.cn

Abstract

In this report, the results of identifying chaotic vibration in a four degree-of-freedom vehicle model by continuous wavelet transform technique are presented. It is shown that the mother wavelet needs to be selected in order to obtain the better transform results. The numeric examples indicate that Mexican hat, Meyer or Morlet mother wavelet may become the best choice for the identification.

I. Introduction

Since the analytical solution of a nonlinear model is usually not available, the numerical analysis and experimental study of chaotic phenomena are the basic ways of investigating critical states of a non-linear system. Therefore the method of identifying chaos from a time history has a great importance. The chaotic state of a system can be indicated with two kinds of ways. One is computation of the dominant Lyapunov exponent. This method is quantitative one and it can prove the existence of chaos conclusively. However it is also a laborious, time-consuming analysis [1]. Another way is qualitative one, for example, observing time-history response, drawing phase portraits, Poincaré maps, bifurcation diagrams or making power spectra analysis and auto-correlation analysis [2]. Since the time history could be complex, several qualitative methods need to be used simultaneously. Because the weak point in existing method, finding a better one is a research topic until now. In a few years ago, it was found that, the characteristic features of a system's chaotic states could be identified by wavelet transform of the system's responses [3]-[5]. The wavelet transform (WT) is a powerful technique to decompose time series in time-frequency domain and to isolate relevant characteristics. Thus this analysis is particularly suitable for the description of non-stationary states and so can be an alternative to the above-mentioned qualitative identification methods.

The aim of this report is to demonstrate the effectiveness of the continuous wavelet transform (CWT) which ensures qualitative identification of chaotic states of the system and show the importance of selection of mother wavelet. Since the unified criterion for selecting mother wavelet in detecting chaos is not yet established, the results could be as a reference for selecting mother wavelet.

II. Continuous Wavelet Transform and the Typical Mother Wavelets

The continuous wavelet transform is a time-scale analysis that consists of expanding signals in terms of wavelets constructed from a single function, the mother wavelet $\psi(t)$, by means of dilations and translations [6]. Thus the CWT of the time function $f(t)$ is defined as

$$W_f\,(a,b) = \langle f,\ \psi\rangle = \frac{1}{\sqrt{a}}\int_{-\infty}^{\infty} f(t)\,\overline{\psi\left(\frac{t-b}{a}\right)}\,dt \qquad a>0 \tag{1}$$

where $f(t)$ is an arbitrary time function, $W_f\,(a,b)$ or $\langle f,\ \psi\rangle$ denotes the CWT of the function $f(t)$, $\overline{\psi\left(\frac{t-b}{a}\right)}$ is the conjugate form of $\psi\left(\frac{t-b}{a}\right)$. The function $\psi(t)$ is used as tick marks to measure signal $f(t)$.

The function $\psi\,(t)$ is referred to as the mother wavelet. It should be noticed that any function can serve as the mother wavelet, as long as it satisfies the following admissibility condition [7]

$$\int_{-\infty}^{+\infty} \frac{\Im\left(\psi\,(t)\right)^2}{|\omega|}d\omega \ < \ \infty \tag{2}$$

where $\Im\,(\cdot)$ denotes the Fourier transform, and ω is the Fourier domain variable. This condition can be described simply in the following way: 1) the mother wavelet function must oscillate and have an average value of zero, and 2) the mother wavelet must have exponential decay and exhibit "compact support."

In definition expressed by Eq. (1), the parameter a represents the scale index, determining the center frequency of the function $\psi\left(\frac{t-b}{a}\right)$. The parameter b indicates the time shifting or translation. The CWT in Eq. (1) takes $f(t)$, a member of the set of square integrable functions of one real variable t in $L^2(R)$, and transforms it to $W_f\,(a,b)$, a member of the set of functions of two real variables (a,b). The low scale a is corresponding to high frequency of $f(t)$ and the high scale a is corresponding to its low frequency.

To make the computation of the CWT, the mother wavelet $\psi(t)$ needs to be selected because the arbitrary choice of the wavelet function and it is possible that, for a same signal $f(t)$, different results of CWT could be produced due to the

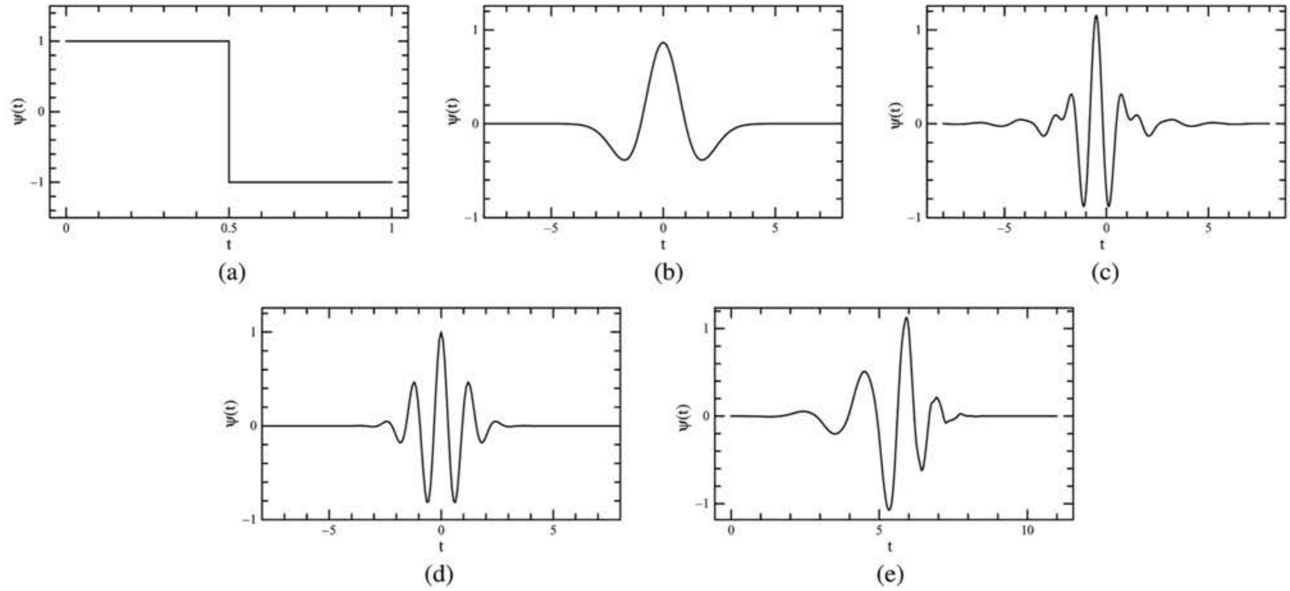

Fig. 1. Mother wavelets: (a) Haar wavelet,(b) Mexican hat wavelet, (c) Meyer wavelet, and (d) Morlet wavelet, (e) Daubechies (db6) wavelet.

selection of mother wavelets. Therefore, the most suitable mother wavelet should be decided to ensure the best transform results. In choosing the mother wavelet, there are several factors which should be considered [8]. According to its shape, the mother wavelet can be divided into a symmetric type, a skewsymmetric type and an asymmetric type by the symmetric property of the function. In this study, these three types of mother wavelet are used and the results for identification of chaotic responses are discussed. In Fig. 1, The wave forms of often used mother wavelet: Haar, Mexican hat, Meyer, Morlet and Daubechies (db6) are presented. The detailed description and properties of these mother wavelets can be found in book [6] and its references.

III. Numerical analysis

A. Nonlinear vehicle model

The four degree-of-freedom vehicle model of the vehicle with non-linear spring forces is shown in Fig. 2 . The notation used is listed in Table I. The model consists of a rigid vehicle body, front and rear unsprung mass, springs and dampers of front and rear suspensions and tires. Suspension is modeled by a non-linear spring and its damping coefficient is assumed to be constant. The suspension springs are assumed to have the following non-linear characteristics [9][10].

$$f_s = k_s \,\mathrm{sgn}(\Delta_s)\ |\Delta_s|^n \tag{3}$$

where f_s is the spring dynamic force, k_s is the equivalent stiffness, Δ_s is the deformation of the spring that can be calculated by the displacement of both extremes of the spring, and $\mathrm{sgn}(\cdot)$ is the signum function. In equation (3), n is an exponent representing non-linearity of the spring and usually ranges between 1 and 1.5. The excitations from the road surface are

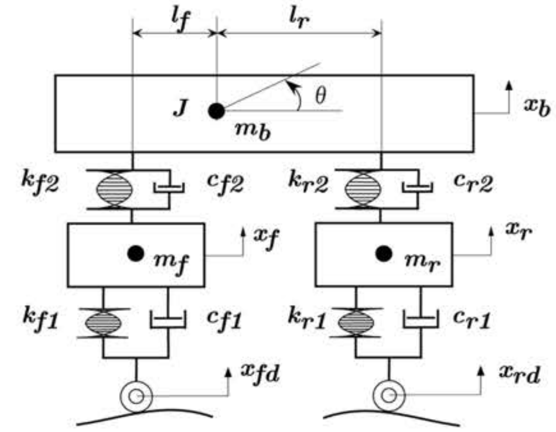

Fig. 2. Half-vehicle model with non-linear spring

TABLE I
NOTATION

m_b	vehicle body mass	J	vehicle body inertia	m_f	front unsprung mass
m_r	rear unsprung mass	l_f	front length	l_r	rear length
k_{f2}	front suspension stiffness	c_{f2}	front suspension damping	k_{r2}	rear suspension stiffness
c_{r2}	rear suspension damping	k_{f1}	front tire stiffness	c_{f1}	front tire damping
k_{r1}	rear tire stiffness	c_{r1}	rear tire damping	$x_b(t)$	displacement of m_b
$\theta(t)$	angular displacement of m_b	$x_f(t)$	displacement of m_f	$x_r(t)$	displacement of m_r
$x_{fd}(t)$	disturbance to the front tire	$x_{rd}(t)$	disturbance to the rear tire		

supposed to be the sinusoid forcing function. The road disturbances for front tires x_{fd}, rear tires x_{rd} are defined as follows.

$$x_{fd} = A\sin(2\pi ft), \qquad x_{rd} = A\sin(2\pi ft + \alpha) \tag{4}$$

where A and f is the amplitude and the frequency of the sinusoid road disturbance, respectively. The parameter α indicates the time delay between forcing functions of front and rear tires. The vehicle body has rigid heave and pitch motions and the unsprung mass has only heave motions. The equation describing the heave motion of the vehicle body can be expressed as [11]

$$\begin{aligned} m_b\ddot{x}_b &= -k_{f2}\,\mathrm{sgn}(D_{bf2})\Big|D_{bf2}\Big|^{n_{f2}} - c_{f2}(\dot{x}_b - \dot{x}_f - l_f\dot{\theta}\cos\theta) \\ &\quad -k_{r2}\,\mathrm{sgn}(D_{br2})\Big|D_{br2}\Big|^{n_{r2}} - c_{r2}(\dot{x}_b - \dot{x}_r + l_r\dot{\theta}\cos\theta) - m_b g \end{aligned} \tag{5}$$

and pitch motion of the vehicle body is given by

$$\begin{aligned} J\ddot{\theta} &= \Big[k_{f2}\,\mathrm{sgn}(D_{bf2})\Big|D_{bf2}\Big|^{n_{f2}} + c_{f2}(\dot{x}_b - \dot{x}_f - l_f\dot{\theta}\cos\theta)\Big] l_f\cos\theta \\ &\quad -\Big[k_{r2}\,\mathrm{sgn}(D_{br2})\Big|D_{br2}\Big|^{n_{r2}} + c_{r2}(\dot{x}_b - \dot{x}_r + l_r\dot{\theta}\cos\theta)\Big] l_r\cos\theta \end{aligned} \tag{6}$$

where

$$D_{bf2} = x_b - \Delta_{sf2} - x_f - l_f\sin\theta, \qquad D_{br2} = x_b - \Delta_{sr2} - x_r + l_r\sin\theta$$

The motion equation of unsprung mass m_f and m_r can be written as follows.

$$\begin{aligned} m_f\ddot{x}_f &= k_{f2}\,\mathrm{sgn}(D_{bf2})\Big|D_{bf2}\Big|^{n_{f2}} + c_{f2}(\dot{x}_b - \dot{x}_f - l_f\dot{\theta}\cos\theta) \\ &\quad -k_{f1}\,\mathrm{sgn}(x_f - \Delta_{sf1} - x_{fd})|x_f - \Delta_{sf1} - x_{fd}|^{n_{f1}} - c_{f1}(\dot{x}_f - \dot{x}_{fd}) - m_f g \end{aligned} \tag{7}$$

$$\begin{aligned} m_r\ddot{x}_r &= k_{r2}\,\mathrm{sgn}(D_{br2})\Big|D_{br2}\Big|^{n_{r2}} + c_{r2}(\dot{x}_b - \dot{x}_r + l_r\dot{\theta}\cos\theta) \\ &\quad -k_{r1}\,\mathrm{sgn}(x_r - \Delta_{sr1} - x_{rd})|x_r - \Delta_{sr1} - x_{rd}|^{n_{r1}} - c_{r1}(\dot{x}_r - \dot{x}_{rd}) - m_r g \end{aligned} \tag{8}$$

In above equations, Δ_{sij} $(i = f, r;\ j = 1, 2)$ indicates the static deformation of the nonlinear springs.

B. Chaotic responses

With the numerical computation, it was found that for some parameter sets, the responses of the system could be chaotic. Fig. 3 shows the Poincaré maps which are from $x_b(t)$, $\theta(t)$, $x_f(t)$ and $x_r(t)$. The strange attractors are exhibited in Fig. 3, which indicates the existence of chaos. Time histories corresponding to Fig. 3 are shown in Fig. 4. By observation, they seem to be varying irregularly. To confirm the responses were chaotic, the method by investigating correlation dimension D_2 and the dominant Lyapunov exponent was implemented [1][12]. To estimate D_2, the Grassberger-Procaccia algorithm [13] [14] was implemented. To create time embedded vectors for calculating dominant Lyapunov exponent, the values of time delay

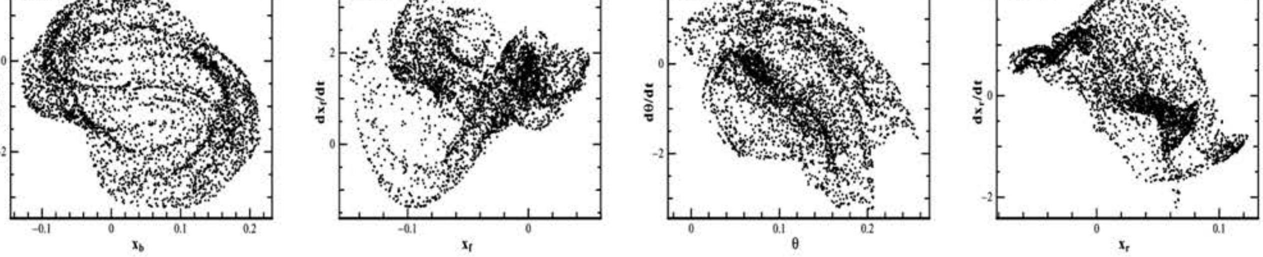

Fig. 3. Poincaré maps of chaotic motion of the system ($c_{f2} = c_{r2} = 500$ kg/s, $c_{f1} = c_{r1} = 10$ kg/s, $A = 0.08$ m, $f = 3.6$ Hz, $\alpha = 150^o$)

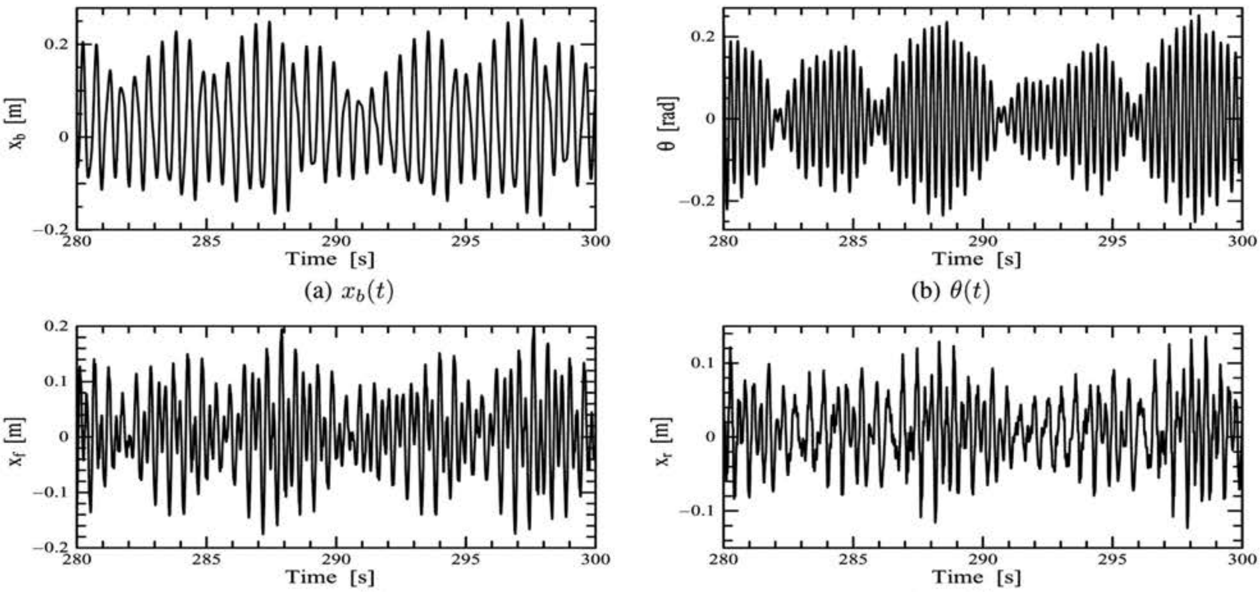

(a) $x_b(t)$ (b) $\theta(t)$

(c) $x_f(t)$ (d) $x_r(t)$

Fig. 4. Time histories of chaotic motion of the system ($c_{f2} = c_{r2} = 500$ kg/s, $c_{f1} = c_{r1} = 10$ kg/s, $A = 0.08$ m, $f = 3.6$ Hz, $\alpha = 150^o$)

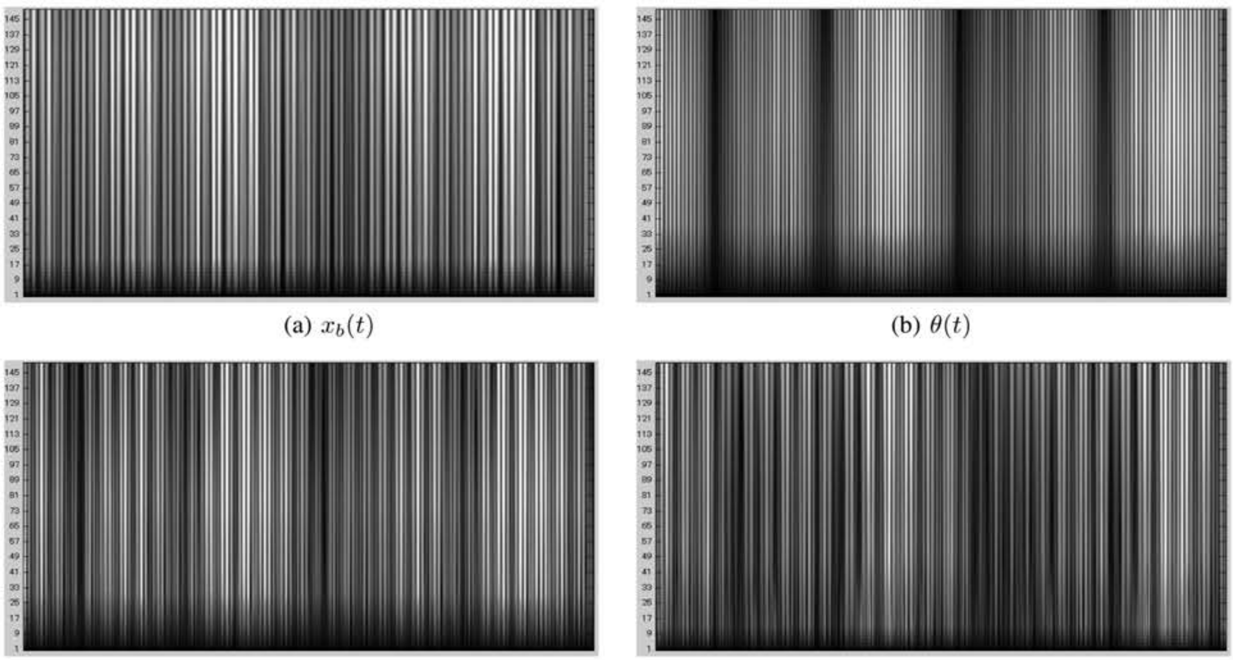

(a) $x_b(t)$ (b) $\theta(t)$

(c) $x_f(t)$ (d) $x_r(t)$

Fig. 5 The results of CWT for the time history in Fig. 4 as Haar wavelet is used.

were determined using average mutual information [15]. The computation gave the values of D_2 for $D_{2x_b} = 1.62$, $D_{2\theta} = 1.47$, $D_{2x_f} = 1.57$, and $D_{2x_r} = 1.56$, respectively. The calculated dominant Lyapunov exponents were $\lambda_{x_b} = 0.65$, $\lambda_\theta = 0.88$, $\lambda_{x_f} = 0.20$, and $\lambda_{x_r} = 0.31$ in the unit of bits/second, which confirm that the responses were chaotic.

C. Results of CWT

The results of CWT for time histories in Fig. 4 are shown in Figs. $5 \sim 9$. The sampling period of the was 0.003 seconds. In these figures, the horizontal axis represents translation b which corresponding to time while the vertical axis represents scale a. The color at each x-y point represents the magnitude of the wavelet coefficient $W_f\,(a,b)$. Larger coefficient is reflected by brighter colors. These CWT coefficient plots are precisely the time-scale view of the original time history.

Fig. 5 exhibits the amplitude behaviors of chaotic time histories of $x_b(t)$, $\theta(t)$, $x_f(t)$ and $x_r(t)$ in the time-scale domain when Haar wavelet is selected as the mother wavelet. It is clear that, the change of pattern along the horizontal axis is indistinct especially for $x_b(t)$. It is also difficult to see any variation along the vertical axis for any specific value of a in the transform results of $x_b(t)$, $\theta(t)$, $x_f(t)$ and $x_r(t)$. Because the variation of pattern in result of CWT will be used as a criterion for possible chaotic motion and it can not be seen at least in this case, the Haar wavelet may not be suitable for the purpose of identifying chaos.

Figs. $6 \sim 8$ are results of CWT using symmetric type of mother wavelet: Mexican hat, Meyer and Morlet. The variation of pattern in theses figures shows the irregular changes in amplitude and frequency of the analyzed time history, which mean the existence of of chaos. Observing Figs. $6 \sim 8$, it may be concluded that the symmetric type of mother wavelet is suitable for tracing the chaotic motion. The results of CWT with Daubechies (db6) which is asymmetric are shown in Fig. 9. The variation of pattern in the results can be observed easily.

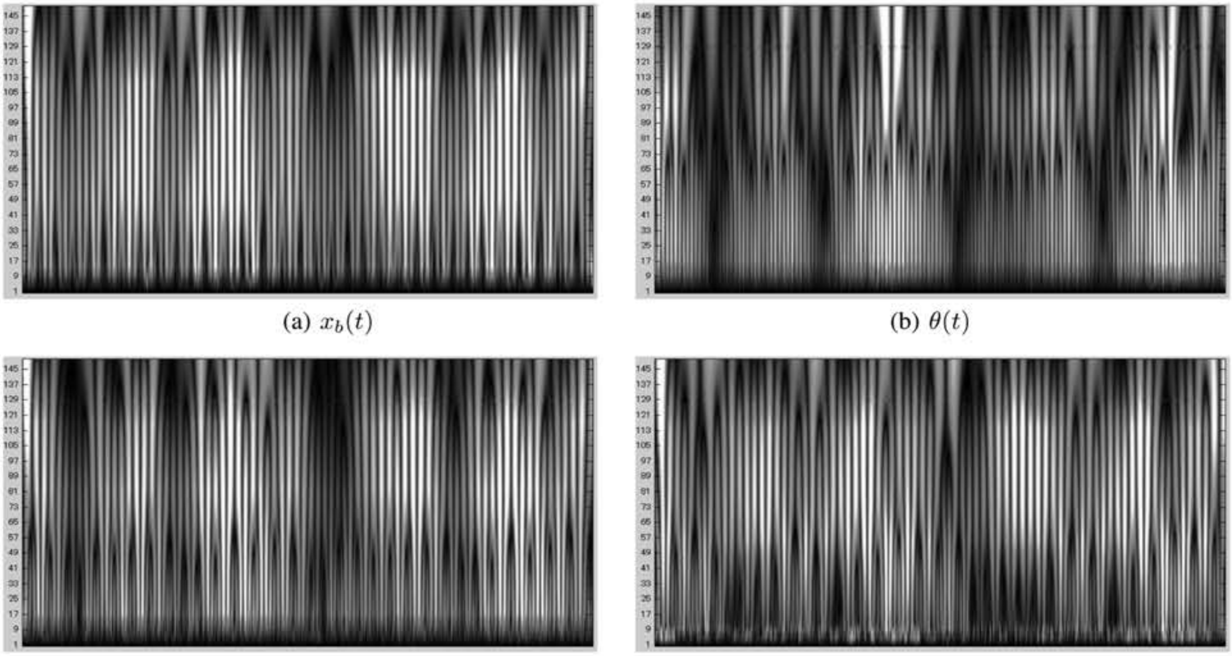

(a) $x_b(t)$ (b) $\theta(t)$

(c) $x_f(t)$ (d) $x_r(t)$

Fig. 6 The results of CWT for the time history in Fig. 4 as Mexican hat wavelet is used.

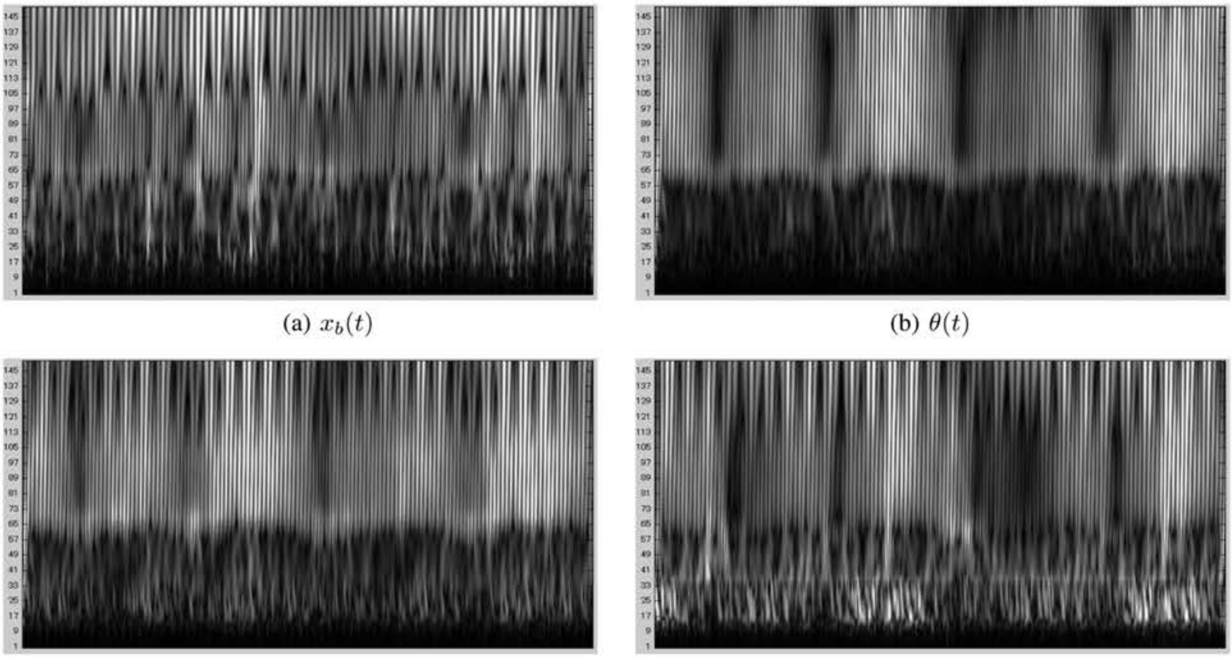

(a) $x_b(t)$ (b) $\theta(t)$

(c) $x_f(t)$ (d) $x_r(t)$

Fig. 7 The results of CWT for the time history in Fig. 4 as Meyer wavelet is used.

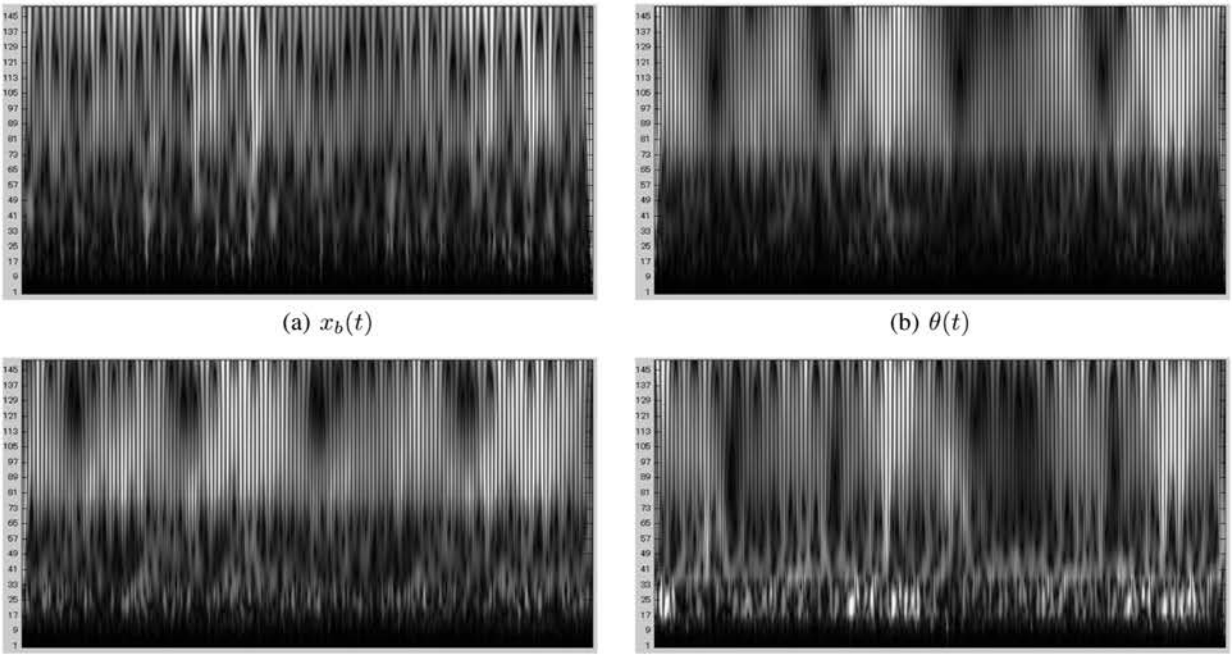

(a) $x_b(t)$ (b) $\theta(t)$

(c) $x_f(t)$ (d) $x_r(t)$

Fig. 8 The results of CWT for the time history in Fig. 4 as Morlet wavelet is used.

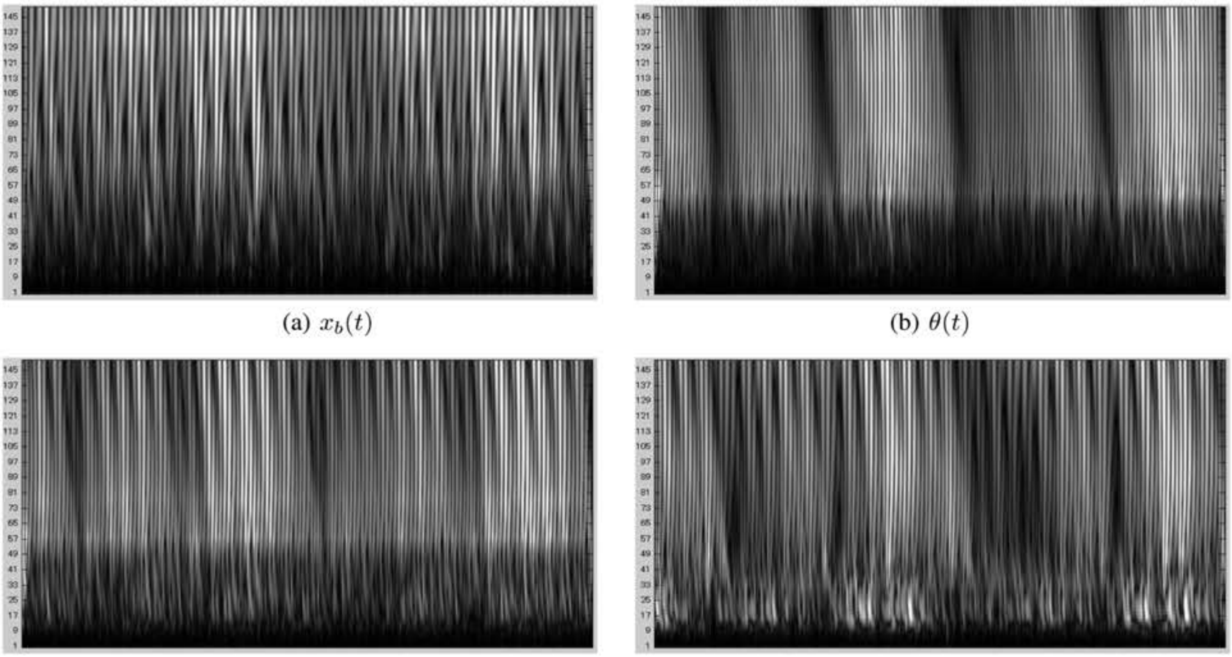

(a) $x_b(t)$ (b) $\theta(t)$

(c) $x_f(t)$ (d) $x_r(t)$

Fig. 9 The results of CWT for the time history in Fig. 4 as Daubechies (db6) wavelet is used.

IV. Concluding remarks

This short report aims at highlighting the effectiveness of using continuous wavelet transform for identifying chaotic response of a four degree-of-freedom nonlinear vehicle mode. The main conclusions deduced from the present investigation are as follows:

1) wavelet analysis of a system's response may constitute an effective qualitative tool for differentiating between the system's chaotic and non-chaotic states;

2) the mother wavelet needs to be selected properly as CWT is implemented for the identifying chaotic motion. The Haar mother wavelet are not suitable for identifying purpose. The symmetric mother wavelet such as Mexican hat, Meyer, Morlet or asymmetric Daubechies (db6) could be a good candidate;
3) the identification of chaotic motion with CWT is conducted by observing variation of pattern in the results. Therefore, it is possible that, for a same result of CWT, different conclusions may be concluded by different observers. The quantitative measurement for evaluating variation of pattern in the result of CWT is needed. This is left for further research.

Acknowledgements

Financial support from Oyama National College of Technology and through Program for New Century Excellent Talents in University of China (NCET-06-0766) are gratefully acknowledged.

References

[1] A. Wolf, J.B. Swift, H.L. Swinney, and J.A. Vastano, Determining Lyapunov Exponents from a Time Series, *Physica*, 16D(1985), pp. 285–317.

[2] F.C. Moon, Chaotic and Factal Dynamics: An Introduction for Applied Scientists and Engineers, 1st ed. John Willey & Sons Ltd., New York, 1992.

[3] B.A. Jubran, M.N. Hamdan, and N.H. S habaneh, Wavelet and Chaos Analysis of Flow Induced Vibration of a Single Cylinder in Cross-Flow, *Int. J. of Engineering Science*, 36 (1998), pp. 843–864.

[4] L.A. Wong, and J.C. Chen, Nonlinear and Chaotic Behavior of Structural System Investigated by Wavelet Transform Techniques, *Int. J. of Non-Linear Mechanics*, 36(2001), pp. 221–235.

[5] W. Glabisz, Analysis of Wavelets in Chaotic States for a One Degree-of-freedom System with Viscoelastic Restraints, *J. of Sound and Vibration*, 258(2002), pp. 633–648.

[6] S. Qian, Introduction to Time-frequency and Wavelet Transforms, 1st ed., Prentice Hall PTR, 2002.

[7] L.M. Bruce, Cl.H. Koger, and J. Li, Dimensionality Reduction of Hyperspectral Data Using Discrete Wavelet Transform Feature Extraction, *IEEE Trans. on Geoscience and Remote Sensing*, Vol. 40, No. 10(2002), pp. 2331–2338.

[8] T. Christopher and P.C. Gilbert, A Practical Guide to Wavelet Analysis, *Bulletin of the American Meteorological Society*, 79(1998), pp. 61–78.

[9] J.C. Dixon, Tires, Suspension and Handling, 2nd ed., Society of Automotive Engineers, Inc., 1996.

[10] A. Moran and M. Nagai, Optimal Active Control of Nonlinear Vehicle Suspension Using Neural Networks, *JSME Int. J.*, Series C, Vol. 37(1994), pp. 707–718.

[11] Q. Zhu and M. Ishitobi, Chaotic Behavior of a Nonlinear Vehicle Model: A Numerical Investigation, Recent Research Developments in Sound and Vibration, Transworld Research Network, S. G. Pandalai (Managing editor), 2002, pp. 363–372.

[12] S. Haykin and S. Puthusserypady, Chaotic Dynamics of Sea Clutter, *Chaos*, Vol. 7(1997), pp. 777–802.

[13] P. Grassberger and I. Procaccia, Characterization of Strange Attractors, *Physical Review Letters*, Vol. 50(1983), pp. 346–349.

[14] H. Takayasu (Edts.), Fractal Science (in Japanese), Asakura Shouten, Tokyo, 1987.

[15] A.M. Feaser and H. L. Swinney, Independent Coordinates for Strange Attractors from Mutual Information, *Physical Review*, A, Vol. 33(1986), pp. 1134–1140.

「受理年月日　2008年9月26日」